Zanardi
Fonderie

AUSTEMPERED DUCTILE IRON AS CAST FATIGUE PROPERTIES

#5

Introduction

This document is designed to familiarize the designer with **as cast fatigue properties of austempered ductile iron materials**. It is a reference document, not to be referred to as a standard.
The data in this document are taken from Zanardi research database, international standards, and technical papers. The content of this informational sheet has to be considered "for information only". The real component design shall be based only upon international standards and/or contractual agreements.

1 Material notes

Austempered Ductile Iron (ADI)

Austempered Ductile Iron (ADI) is obtained by heat-treating an alloyed ductile iron, casted with a special preconditioning of the metal bath.
The matrix structure consists predominantly of ferrite and acicular austenite. The obtained matrix is called "ausferritic" which offers the combination of high fatigue resistance, toughness, wear resistance, lightness and extensive freedom in designing components together with significant machining properties.

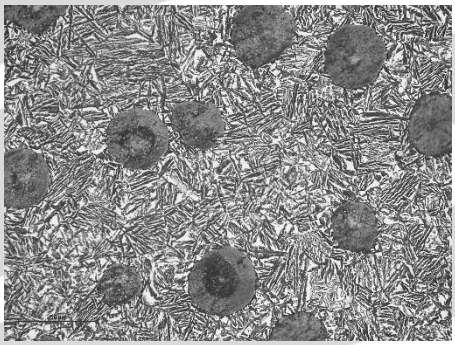

Isothermed Ductile Iron (IDI)

Perferritic Isothermed Ductile Iron (IDI) is a material from a process consisting of austenitizing an unalloyed ferritic ductile cast iron and quenching in a salt bath. The following quenching above martensite start temperature transforms austenite into pearlite due to the fast cooling rate imposed by low salt bath temperature. The characteristic microstructure of IDI contains a ferritic network with very fine pearlite in between. IDI therefore represents an intermediate state between the lowest austempered ductile iron (ADI) grades and pearlitic ductile iron. In contrast to ADI, no additional alloying elements like Ni, Cu or Mo are necessary to achieve an IDI microstructure, as the formation of pearlite is a desired effect.

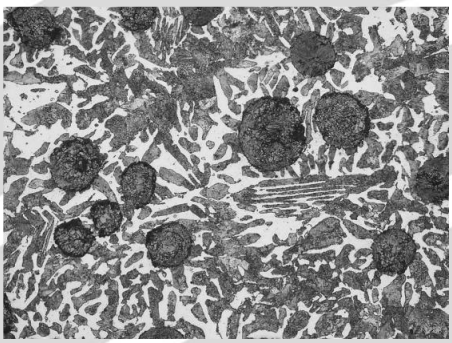

2 As cast Fatigue properties

ADI, IDI & DI high cycles fatigue properties

Typically, fatigue loaded components must be assessed against notch fatigue, because crack initiation occurs at stress raisers. Classical approaches for fatigue design are based on the elastic stress concentration factor K_t, which can be used as fatigue reduction factor in cases when full notch sensitivity is predicted or, alternatively, can be corrected by a notch sensitivity index *q* when partial notch sensitivity is likely to occur. For a given material, the *q* factor can be calculated as a function of the notch tip radius: large radii (on the order of some millimeters) lead to full sensitivity, while lower radii involve partial notch sensitivity, i.e. the reduction factor at fatigue limit is lower than K_t.

However, when the notch radius tends to zero K_t-based approaches to fatigue limit analysis (even though corrected by the sensitivity index *q*) do not hold true any longer because stresses growths to infinity. It is well known that Fracture Mechanics concepts must be adopted to attack this problem.

Kitagawa and Takahashi first analyzed experimentally the threshold conditions of a crack. The results of their experiments can be summarized in the diagram reported in picture 1, where, as an example, the threshold range of the gross stress $\Delta\sigma_{g,th}$ of a crack centered in an infinitely wide plate and subjected to mode I loading is presented.

When the crack is sufficiently long, the threshold condition is given by the threshold value ΔK_{th} of the linear elastic stress intensity factor ΔK_I at the crack tip. However, as the crack size is reduced, the threshold stress becomes lower than that predicted by the Linear Elastic Fracture Mechanics and becomes equal to the plain material fatigue limit $\Delta\sigma_0$ as the crack length is further reduced. The limitation of applicability of the constant stress and constant stress intensity factor criteria is schematically represented by the material parameter a_0 introduced by El Haddad. This is due to interactions between short cracks and microstructure, thus the hypothesis of continuum is no longer satisfied. The slope of fracture mechanics line is equal to 0,5 for metals.

In recent years the diagram has been extended to include finite size components and different notch geometry.

Picture 1 - Fatigue limit of cracks

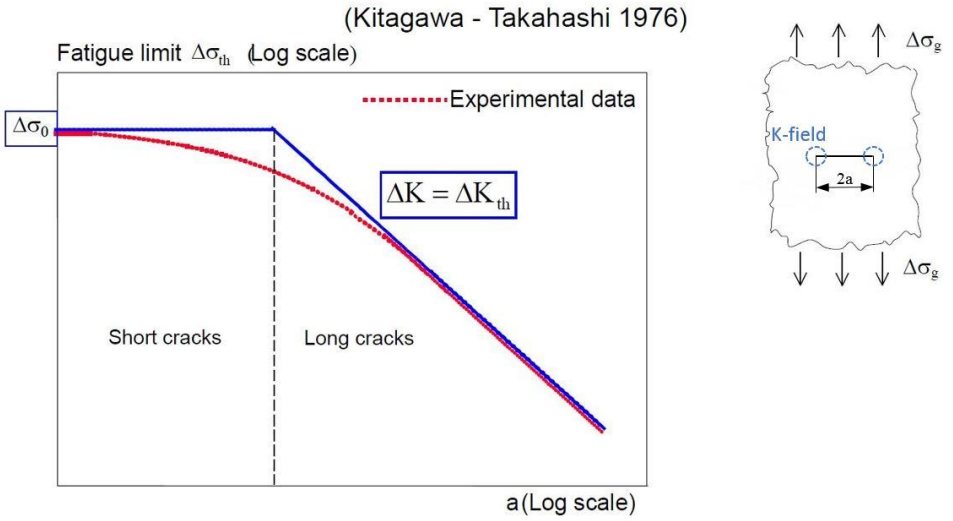

K_{th} is a material property, i.e. the threshold stress field for crack propagation

Picture 2 - Advanced fatigue assessment, summary

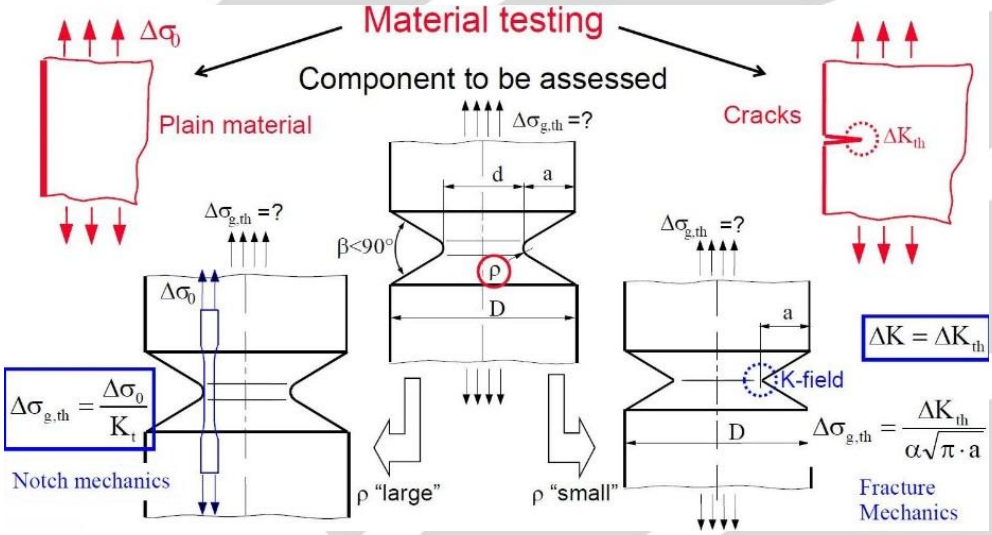

Fatigue behavior of FDI, PDI, IDI and ADI1050 has been characterized experimentally by means of rotating bending tests of smooth specimens, in order to derive the plain fatigue limit, and by means of sharply notched specimens, in order to define the crack threshold ΔK_{th}. For each material, specimens have been obtained machining Y block samples having rel. w.t. 25-50-75 mm.

All theoretical estimations indicate a sharp behavior of the specimens, i.e. the 0.1mm notch tip radius is ineffective on the fatigue strength, which can be assimilated to that of notch having a zero notch tip radius. In fact, because short non propagating cracks exists at the tip of notch under threshold conditions, the notch can be considered equivalent to a crack having the same depth.

When applying El Haddad equation, the length parameter a_0 was input equal to zero because the notch depths involved in the analysis results at least six times longer than a_0.

Picture 3 - Specimen's geometry and experimental procedure

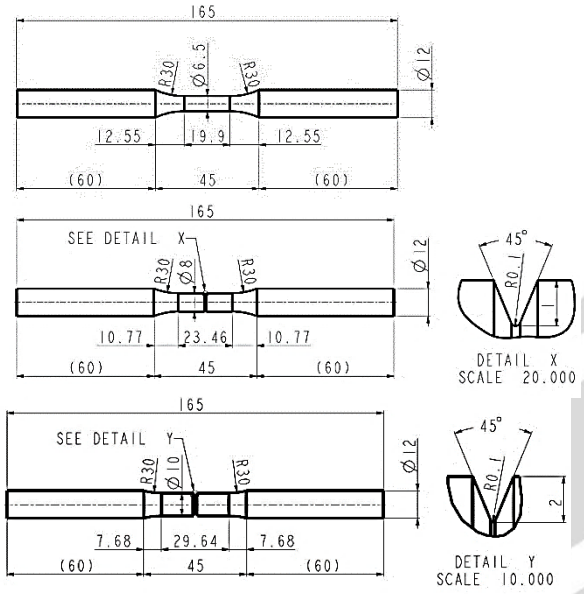

- Rotating bending test (R=-1)
- Zwick Roell UBM200 testing machine
- Test frequency f=100 Hz
- Brownlee-Hodges-Rosenblatt short stair case (run out $5 \cdot 10^6$ cycles); p.s. 50%, confidence level 95%
- Specimens machined from separately cast Y25, Y50 and Y75 blocks
- Test setup according to ISO 1143
- Definition of generalised Kitagawa-Takahashi diagram

Table 1 summarizes the material characterization and the experimental results referred to the gross section of the specimens. Plain fatigue limit is given in terms of nominal stress amplitude (half of the range maximum-minimum applied stress). The crack threshold range ΔK_{th} was calculated by fitting the data relevant to the V-notched specimens by means of the El Haddad equation.

Table 1 – Material characterization and experimental results

Material	Microstructure	Rel. w.t. [mm]	HBW	$HV_{0,5}$	Nod. count [Nod/mm²]	D_{nod} avg. [µm]	D_{nod} max. [µm]	$\sigma_{Ag50\%}$ [MPa]	ΔK_{th} [MPa·√m]	a_0 [mm]	8-1-0,1		10-2-0,1	
											$\sigma_{th50\%}$	$\alpha^2 a$ [mm]	$\sigma_{th50\%}$	$\alpha^2 a$ [mm]
DI	Ferritic	25	156	179	330	21	37	**279**	**12,7**	0,164	78	2,09	38	8,78
		50	145	179	170	28	45	**278**	**14,3**	0,213	94	2,02	41	9,05
		75	161	182	125	32	62	**265**	**16,5**	0,310	108	2,10	48	8,61
DI	Pearlitic	25	250	289	260	22	42	**350**	**17,7**	0,204	103	2,07	57	8,75
		50	239	298	150	29	50	**315**	**20,1**	0,325	143	2,00	55	8,51
		75	244	294	145	29	54	**327**	**19,8**	0,291	129	2,09	56	8,94
IDI	Pearlitic-ferritic interconnected	25	255	301	280	21	38	**390**	**16,0**	0,133	93	2,05	53	8,76
		50	249	300	180	27	47	**321**	**18,8**	0,271	122	2,06	55	8,42
		75	242	305	135	31	60	**314**	**19,5**	0,308	124	2,06	58	8,73
ADI1050	Ausferritic	25	346	395	300	20	34	**441**	**20,3**	0,168	122	2,00	66	8,12
		50	349	412	165	29	50	**362**	**24,7**	0,370	156	2,03	73	9,01
		75	354	420	110	34	70	**356**	**23,1**	0,337	141	2,07	73	8,37

Graphic 1 - Experimental results, schematic

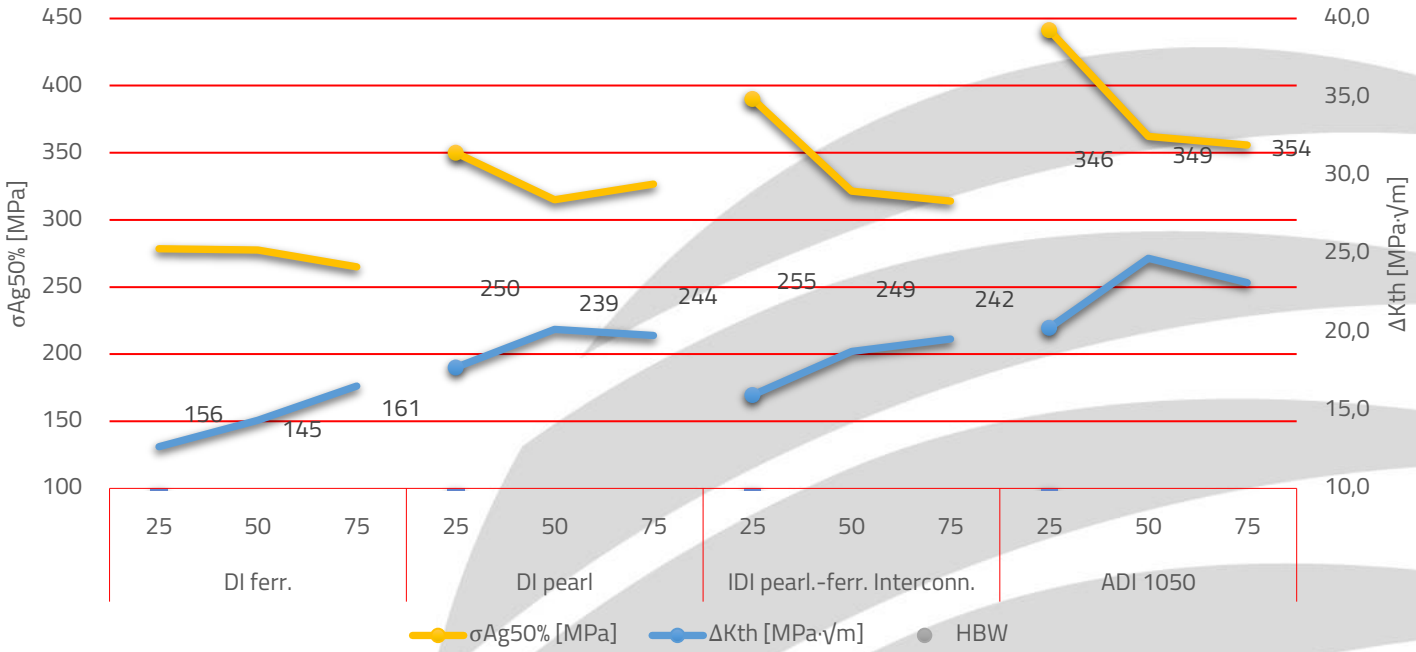

Experimental evidence shows that:

- for a given material: the higher is rel. w.t. (HBW is almost constant through the thickness, whereas nodule size increases), the lower is plain fatigue limit $\sigma_{Ag,50\%}$ and the higher is crack threshold ΔK_{th};
- between material: the higher is Brinell hardness HBW, the higher are both plain fatigue limit and crack threshold ΔK_{th};
- heat treatment improves fatigue performances (DI ferritic to IDI, DI pearlitic to ADI).

Picture 4 - Kitagawa-Takahashi diagrams for rel. w.t. 25 mm, trend of results

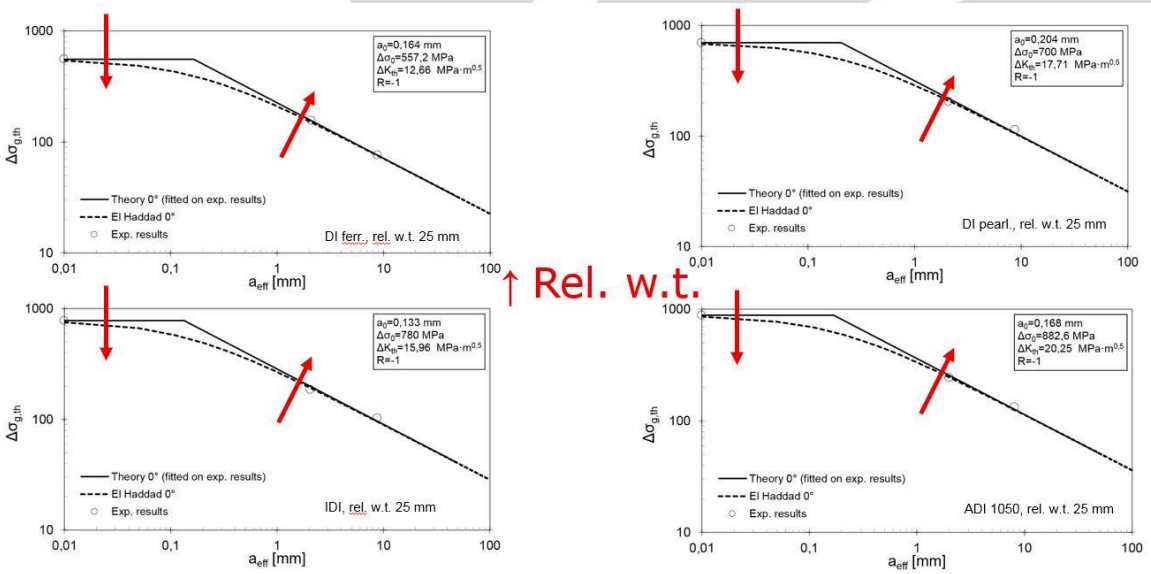

Regarding the plain fatigue limit, according to Murakamy research work, graphite nodule acts as crack initiation: the higher the size the lower is plain fatigue limit. As shown by the diagram, this effect is more significant for high strength materials.
Furthermore, plain fatigue limit doesn't represent a limit for crack initiating, but a propagation threshold for short cracks emanating from the graphite nodules.
Regarding the crack threshold ΔK_{th}, coarse microstructure typical of large rel. w.t., exhibits high misorientation angle grain boundaries, which represent a very strong barrier for crack propagation: as confirmed by experiments, the higher is the thickness, the higher is crack threshold.

State of the art of ADI high cycles fatigue properties in case of "as cast" surface obtained with green sand process

Among the many parameters that influence the fatigue resistance of a component, surface conditions play a key role since they can cause a significant decay of fatigue performances. In general, most of the castings obtained by green sand process, operate in raw condition except for connection or coupling surfaces.
The development of design tools able to describe the as-cast surface quality conditions is very challenging. The following experimental approach based on Linear Elastic Fracture Mechanics (LEFM) is proposed.

The knowledge about "as cast" surface effect on fatigue resistance of DI iron and in particular of ADI iron, is currently based on a limited experimental works. However, the great variability of surface quality and complexity of defects shape makes the formulation of theoretical models very hard. For this reason, the aim of this paper is only to present a possible approach for fatigue design of ADI castings and to give some information, complementary to those available on international material standards. Data about materials properties comes from a limited research program and/or literature, in some cases they are only hypothesis to be considered for future research.
The typical "as cast" surface we can obtain by pouring DI in green sand mould (see picture 5), consist in a multilayer structure as follows:

- casting skin is the first layer in contact with the mould; it is few micrometers thick and free of graphite nodules. Due to the high initial cooling rate at the interface metal-mould, the crystal lattice of skin contains a lot of dislocations, vacancies, interstitials, grain boundaries, etc. The average surface roughness is Ra = 12,5 µm;
- a transition layer ≈0,8 mm thick, just below the skin, connecting it with bulk material. In general, depending on iron composition, it mainly consists in a fine and compact ferritic structure, with few coarse graphite nodules; this is due to the interaction metal-mould. The layer also contains a lot of small discontinuities having size much smaller than its material constant a_0 layer, which is unknown at this step; since they cannot be avoided, we can consider them part of this structure;
- defects, such as sand inclusions, slag inclusions, gas bubble, cracks, porosity, etc. or dents. In general, their size is bigger than the material constant a_0 layer and their dimension can extend to the bulk material having the known material constant a_0 bulk.

Picture 5 – Typical characteristics of the as-cast surface of all ductile iron grades

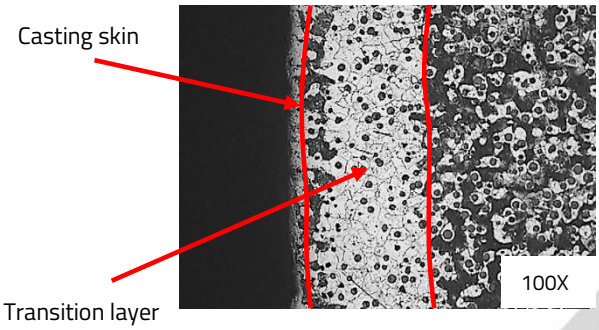

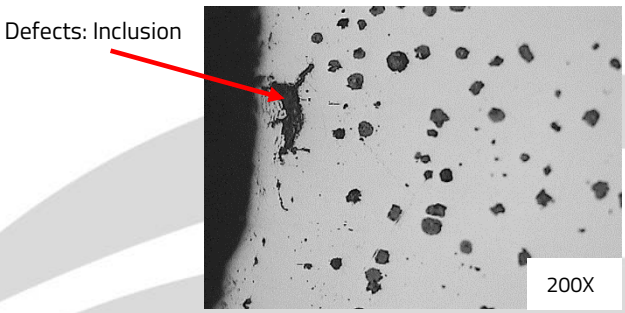

We introduced the definition "sound as cast surface", according to previous definition and excluding defects; this is the best you can get from a normal green sand process. The characteristics, as well as mechanical properties, of the "sound as-cast surface" are common to all ductile irons.
Starting from this baseline, the goal is to estimate fatigue limit when an additional defect, such as slag inclusion, sand inclusion, gas bubble, deep crack and dent, is given.
In presence of defect, fatigue limit is leaded by the condition of non-propagation of cracks emanating from it, due to local stress peak. The stress concentration factor K_{tg} (referred to gross section) has not to be considered, even if the defect is round shaped, because its surface is not smooth in any case. We have supposed that size of defects is small if compared with gross cross section.

According to LEFM approach, Kitagawa-Takahashi generalized experimental diagram (see graphic 3) has been developed for ADI 1050; in particular, the diagram integrates the results of both machined (plain) and as-cast surface condition in a single design tool.

LEFM theory

Starting from the Stress Intensity Factor equality [1]:

$$\alpha^2 a = \frac{1}{\pi} \cdot \left(\frac{K_I}{\sigma_g} \right)^2 \qquad (1)$$

and replacing KI with the expression, valid for surface crack, proposed by Murakami [2]:

$$K_I = 0{,}65 \cdot \sigma_g \cdot \sqrt{\pi \sqrt{Area_p}} \qquad (2)$$

the following equation can be obtained:

$$\alpha^2 a = k \cdot \sqrt{Area_p} \qquad (3)$$

being the constant k equal to 0,42 and $Area_p$ the projected cross section area, normal to main stress direction, of the smooth contour of defect (see picture 6) [2]. Depending on the kind of defect we are considering (slag inclusion, sand inclusion, etc.), and in particular on how it can be represented, the constant k can be slightly modified.

It applies to inclusions, gas bubbles, cracks (last ones can also be treated with analytic expressions from fracture mechanics), etc.

It is also valid for dents, but in this case the calculation of $\alpha^2 a$ is needed only to reorder the data in Kitagawa Diagram: in fact, due to their shape, the effect of dents should be considered via K_{tg}, being mostly in full notch sensitivity conditions. However, the effect of dents is a very complex matter to be investigated: it depends on the intensity of impact, the local compression generated, relaxing of compressive stress after heat treatment, possible graphite nodule breakage, cracks formation, presence of defects, etc.

Picture 6 – Arbitrarily shaped defect and its equivalent area "$Area_p$"

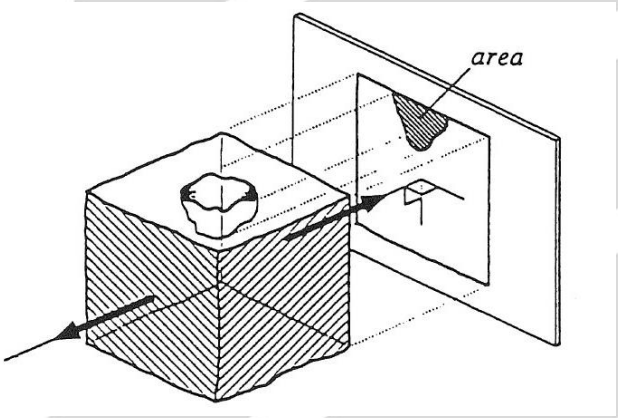

Fatigue tests on ADI1050 un-machined round bar samples

Experiments, consisting in estimation of fatigue limit using Locati method, were carried out in rotating bending (R = -1) on 52 un-machined ADI round bar specimens (see picture 7), not shot-blasted after heat treatment; specimens have been collected from different batches during one year production.

Locati method, as known, is based on Miner cumulative damage hypothesis and implies the knowledge of three Wohler curves at least, in this case for as cast conditions. In general, the method is less accurate than Stair Case, but it allows to get one fatigue limit for each defect, that is, for one sample. However, using Stair-Case method for as cast condition, fatigue limit obtained is representative of a given defects distribution: this means that scattering due to material and defects are coupled together.

All 52 specimens, tested in rotating bending, failed due to a single sand inclusion defect: no slag inclusions have been observed. When crack initiation has been encountered at parting line fins, results obtained haven't been considered.

All experimental results are reported in table 2.

Picture 7

a) un-machined specimen

b) rotating bending test rig

Table 2 - Experimental fatigue limits (R = -1, P.S. 50%) according to Locati method, $\alpha^2 a$ according to Equation 3

Batch	Sample n°	$\Delta\sigma_{0\ PS50\%}$ [MPa]	$\sqrt{Area_p}$ [mm]	$\alpha^2 a$ [mm]	Batch	Sample n°	$\Delta\sigma_{0\ PS50\%}$ [MPa]	$\sqrt{Area_p}$ [mm]	$\alpha^2 a$ [mm]
1	1	332	0,99	0,46	4	28	288	1,17	0,53
	2	372	0,51	0,25		29	346	0,95	0,44
	3	394	0,61	0,29		30	358	0,85	0,40
	4	320	1,09	0,50		31	364	1,23	0,56
	5	304	1,05	0,48		32	390	0,57	0,28
	6	288	0,85	0,40		33	298	0,58	0,28
	7	400	0,45	0,23		34	350	1,06	0,48
	8	414	0,40	0,21		35	322	0,97	0,45
	9	318	1,04	0,48	5	36	352	0,84	0,39
	10	298	1,19	0,54		37	312	0,87	0,41
2	11	282	0,84	0,39		38	322	0,75	0,36
	12	318	0,73	0,35		39	356	0,65	0,31
	13	318	0,77	0,36		40	302	2,04	0,90
	14	340	0,81	0,38		41	342	0,76	0,36
	15	308	1,69	0,75		42	328	1,34	0,60
	16	274	1,23	0,56		43	352	0,85	0,40
3	17	284	1,17	0,53	6	44	358	0,78	0,37
	18	288	0,92	0,43		45	288	1,52	0,68
	19	268	1,43	0,64		46	312	0,72	0,34
	20	386	1,04	0,48		47	304	0,87	0,40
	21	406	0,62	0,30		48	344	1,70	0,75
	22	318	2,65	1,42		49	346	0,81	0,38
	23	490	0,76	0,36		50	344	0,74	0,35
	24	350	0,66	0,31		51	314	1,39	0,62
	25	402	0,54	0,26		52	344	1,19	0,54
	26	352	1,02	0,47					
	27	360	1,39	0,62					

Picture 8 - Typical sand inclusions at fatigue crack initiation point

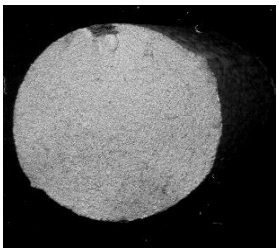

Sample 16
$\sqrt{Area_p}$ = 1,23 mm
$\alpha^2 a$ = 0,56 mm
$\Delta\sigma_{0\ R=-1,\ P.S.50\%}$ = 274 Mpa

Sample 31
$\sqrt{Area_p}$ = 1,23 mm
$\alpha^2 a$ = 0,56 mm
$\Delta\sigma_{0\ R=-1,\ P.S.50\%}$ = 364 Mpa

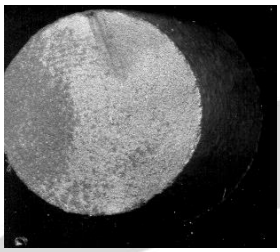

Sample 47
$\sqrt{Area_p}$ = 0,87 mm
$\alpha^2 a$ = 0,40 mm
$\Delta\sigma_{0\ R=-1,\ P.S.50\%}$ = 304 Mpa

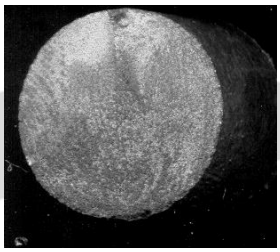

Sample 48
$\sqrt{Area_p}$ = 1,70 mm
$\alpha^2 a$ = 0,75 mm
$\Delta\sigma_{0\ R=-1,\ P.S.50\%}$ = 344 Mpa

Regression analysis of experimental figures, once the crack threshold value ΔK_{th} of the bulk have been imposed, allows to draw the as cast Kitagawa-Takahashi experimental diagram (see graphic 2).
Extrapolating to α^2a (effective defect size) equal to zero, the horizontal line represents the as-cast fatigue limit without defects.
Kitagawa-Takahashi diagram allows defining material constant a_0 layer. In particular, it shows that the effect of as cast surface on fatigue limit reduction is concentrated at the transition between short cracks and long cracks; in fact, considering defects, sharp notches or long cracks, each having effective depth α^2a value much higher of a_0 layer , doesn't matter if the surface is, or not, in machined conditions: fatigue limit will be the same for both machined or "as cast" surfaces, being calculated using ΔK_{th} of bulk material.
Once the effective defect depth α^2a is known, Kitagawa Diagram allows us to estimate the fatigue limit at probability of survival of 50%.
It is worth noting that scattering at transition between short and long cracks is quite large, as expected; this is a reasonable result considering that experimental data comes from six different batches over one year production and they have been obtained using Locati method.

Graphic 2 - As cast Kitagawa-Takahashi experimental diagram

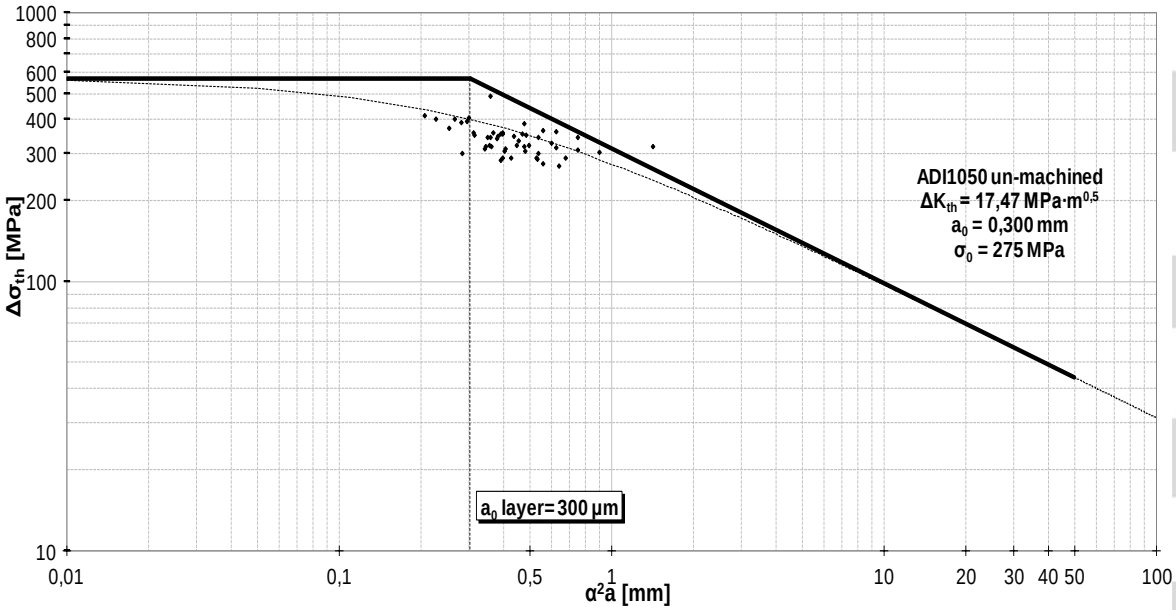

Looking at Generalized Kitagawa diagram (see graphic 3), further considerations can be done. K_L parameter represents the reduction coefficient plain-to-as-cast surface. According to this approach, as-cast surface without defects can be treated as a different material having its own mechanical properties.
Defects having effective size lower than a_0 layer do not cause any further decrease of the fatigue limit; on the other hand, it's evident that larger defects contribute to an extra reduction of the fatigue limit, reaching an asymptotic overall value in the range of K_L 2,5-3, being this range significant for casting skin that incorporates inclusions having schematic size of 2x2 mm (typical for green sand foundry process).

Graphic 3 - Kitagawa-Takahashi generalized diagram for ADI 1050

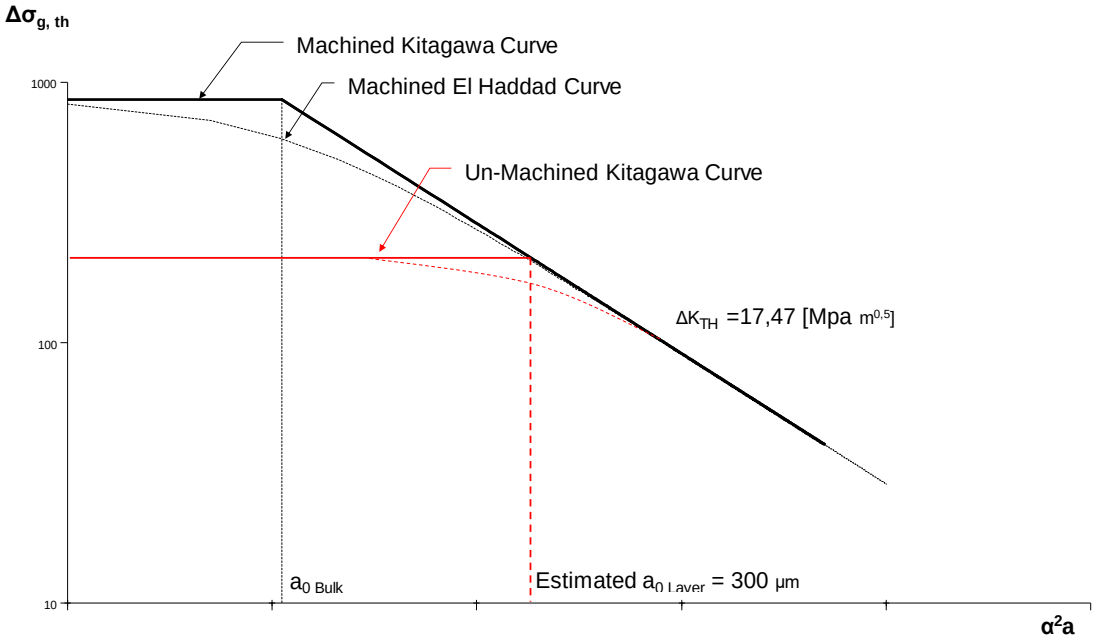

Conclusion

In case of sand inclusion, Kitagawa model for ADI 1050 represent a powerful design tool for the estimation of fatigue limit at probability of survival of 50% once the effective defect depth $\alpha^2 a$ is known.
Designers have to bear in mind that K_L factor applies for rotating bending fatigue limit at 50% probability of survival, that is before estimating different probability of survival, load conditions, size effect, etc.
Kitagawa model can be extended to other kind of defects, to all ADI, IDI, DI and shot-blasted conditions.
Fatigue performances of "as cast" surface can be improved of about 30% by shot peening, at fatigue limit: in fact, at higher stress level as in the upper part of finite lifeline, relaxation of compressive residual stresses occurs and this is due to local plasticization of the material.

References

[1] Atzori, B., Lazzarin, P.,Meneghetti, G. (2005). A unified treatment of the mode I fatigue limit of components containing notches or defects. International Journal of Fracture 133, p. 61-87.
[2] Murakami, Y. (2002). Metal Fatigue: Effects of Small Defects and Nonmetallic Inclusions. (Edited by Y. Murakami), Elsevier, Oxford, p. 16-19.